

Characterization of hydroxyapatite coating on Mg-1%Zn alloy for implant application

M. Esmail*, O. R. M. Khalifa*, E. A. Al Hamed*, A. Kassab*.

* Chemistry department, Faculty of Girls for Arts, Science and Education, Ain shams university.

Abstract

Most conventional orthopedic implant used for joint and bone fractures consist of metallic biomaterials with polycrystalline microstructures that exhibit high hardness, good corrosion resistance, excellent fatigue and wear resistance.

Alternatively, to avoid post extraction of the implant, intensive efforts are being made in recent years to develop new classes of so called “biodegradable implant composed of non-toxic materials that become reabsorbed by the human body after a reasonable period of time.

We use Mg alloys since they have poor corrosion resistance in the body environment. i.e Mg-1%Zn alloy. Zinc improves the mechanical properties of the magnesium alloys and does not show any side effects on the human body.

This investigation shows ways of improving corrosion resistance of this alloys by electrodeposition of hydroxyapatite (HA), hydroxyapatite with high concentration of phosphate (HAP), hydroxyapatite with high concentration of calcium (HACa) and hydroxyapatite with high concentration of both phosphate and calcium (HAPCa) as a bio-compatible coating. The coating improves the corrosion protection of Mg-1%Zn alloy. The corrosion protection follows the sequence HAPCa > HACa > HAP > HA.

Key Words: Mg-1% Zn, Hydroxyapatite, Phosphate and Calcium Nitrate

Corresponding author: marwa mohammed mohammed

E-mail: marwaesmail4m@yahoo.com.

I- Introduction

Magnesium is the fourth most abundant cation in the body equal about 1 mol (24g) in an adult human body and over 60% is accumulated in bone and teeth that concentrated on the hydrated surface layers of apatite crystals instead of incorporated into the lattice structure of bone crystals [Wenhao Wang et al]. Among all calcium phosphate hydroxyapatite (HA), $\text{Ca}_{10}(\text{PO}_4)_6(\text{OH})_2$ is the most extensively used biocompatible ceramic materials for bone tissue, as its chemical composition is similar to the bone mineral phase [A. Farzadi et al]. An appropriate alloying composition can improve the corrosion resistance, mechanical properties and the ease of manufacture of Mg-based materials. Zn is one of the most abundant elements in the human body and has basic safety for biomedical applications. Zn helps to overcome the harmful corrosion impurities that might be present in the Mg alloys. Mg-1%Zn produced less hydrogen than many other binary Mg alloys in simulated body fluid (SBF) [S.M. Abd El Hallem et al]. The degradation rate of Mg based implants is too rapid in the body fluid environment to keep mechanical integrity before the diseased or damaged bone tissue healed. Surface modification is generally accepted as an effective approach to delay the degradation rate of Mg based implants during the service period [Y. Xiong et al]. Compared to the

other commonly used artificial implant materials, the mechanical properties of Mg alloys are more similar to human bone, which avoid the stress shielding [G. Hu et al]. Alloying of Mg with non-toxic and essential metals such as Zn, this biomaterial is expected to present optimal biocompatibilities, despite the interesting mechanical properties requires additional surface protection strategies to meet the requisites for biomedical applications[S.M. Abd El Hallem, Y. Yan, J.A.del Valle, Y. Song et I]. The homeostasis provided by the adjacent tissues to the implanted materials i.e compensation of ions imbalance from alloys dissolution and corrosion products precipitation [D. Vojtech et al], is an important factor to have in consideration in invitro assays. This has not yet been considered for the invitro corrosion studied of Mg-Zn alloys [J. Kubasek, ch, J. Kub'asek, M. S. Dambatta, Jamesh, M et al]. In our research, we study electrodeposition of four bathes on Mg- 1% Zn alloy and compare the results of the four bathes.

II- Experimental techniques

II.1 - Materials

Mg-1%Zn alloy sheets

Specimens of Mg-1% wt Zn is cutting with dimensions 2x2 cm and 5mm thickness. The alloy with a chemical composition of Mg-1%Zn is prepared from pure Mg and Zn using a laboratory resistance furnace. The melt is transferred to a semi-continuous casting machine at 900°C

II.2- Preparation of Electrolyte Solution:

Electroplating bathes include $\text{Ca}(\text{NO}_3)_2 \cdot 4\text{H}_2\text{O}$ as the calcium ion source, ammonium di-hydrogen phosphate $\text{NH}_4\text{H}_2\text{PO}_4$ as the phosphate ion source, sodium nitrate NaNO_3 to increase conductivity, hydrogen peroxide (H_2O_2) to erase in table (1).

Table (1): Chemical composition of coating baths:-

Coat	HA	HAP	HACa	HAPCa
Composition				
$\text{Ca}(\text{NO}_3)_2$	9.90 g/l	9.90 g/l	11.00 g/l	11.00 g/l
$\text{NH}_4\text{H}_2\text{PO}_4$	2.87 g/l	4.00 g/l	2.87 g/l	4.00 g/l
NaNO_3	1.27 g/l	1.27 g/l	1.27 g/l	1.27 g/l
Na_3PO_4	2.00 g/l	2.00 g/l	2.00 g/l	2.00 g/l
H_2O_2	20.00 ml/l	20.00 ml/l	20.00 ml/l	20.00 ml/l

The optimum conditions are pH 7.4 and temperature 37°C. Fixed potential was set to 1.4V and time 30min. The circuit is connected so that, the magnesium alloy substrate became negatively charged (as cathode).

Table (2): Chemical composition of simulated body fluid (SBF):-

Chemicals	NaCl	KCl	CaCl_2	NaHCO_3	MgSO_4	KH_2PO_4	Na_2HPO_4	Glucose
Wt.(gm/l)	8.8	0.4	0.14	0.35	0.2	0.1	0.06	1

The specimens are mechanically polished abraded to 2000 grit finish with SiC paper, the specimen are carefully rinsed in distilled water, dried with hot dry air and stored in a desiccator if not

immediately examined. The samples are weighed before and after plating and the difference in weight is calculated.

II.3- Coating process:

The cleaned samples are coated electrochemically for a definite time 30 min at room temperature. Agitation of the solution took place at 250-500 r.p.m. we use four baths for the deposition of coat, HA, HAP, HACa and HAPCa.

The optimum condition for coating is done for the bath HA then, use the same conditions for the other three bathes in order to compare between them.

II.4- Surface characterization of the coatings:

The properties of electro-plating coating as plated and after immersion in simulated body fluid (SBF) (table 2), for 2 and 4 weeks at 37⁰C, are investigated. Scanning electron microscope (SEM), FTIR of coatings, X-ray diffraction (XRD) and EDAX are used for investigation.

II.4.1- Scanning electron microscope (SEM):

SEM (Quanta 250 FEG, Taiwan) is used to demonstrate the surface morphology. The examination is carried out on different samples employing an accelerating voltage of 30kv. Samples are mounted using carbon paste to ground them. The results are obtained as computer printout.

II.4.2- Fourir-Transform Infrared Spectroscopy (FTIR):

FTIR spectra are obtained using pearl bruker IFS 125 HR and are recorded in the 4500-400 cm⁻¹ region with 0.0024 cm⁻¹ resolution by using KBr pellet technique

II.4.3- X-ray Diffraction (XRD):

An X-ray diffractometer (D8 ADVANCE X-RDIFRACTOMETER, Germany) with copper target and nickel filter is used for identification of the phases, amorphous and crystalline structure of the deposits.

II.4.4- Corrosion Resistance:

Electrochemical study tests are carried out using a classical three electrode cell with Pt as counter, Ag/AgCl electrode as reference electrode, and the samples as working electrode. The potentiodynamic curves are obtained using a model CHInstrument.

III- Results and discussion:

The surface morphology of the as deposited coating is shown in Fig (1). Figure 1(a) show dendritic crystal and indendritic second phase is present with a grain size 8.50 μm. Fine flake- like particles are observed on the surface of Fig 1(b) with white spot and its grain size is 7.10 μm.

Fig 1(c) shows flake-like particles, some flakes have white colour (means deposition of calcium) and others have black colour with grain size 5.30 μm. For (HAPCa), figure 1(d) shows plate-like morphology containing white spots with grain size 2.19 μm.

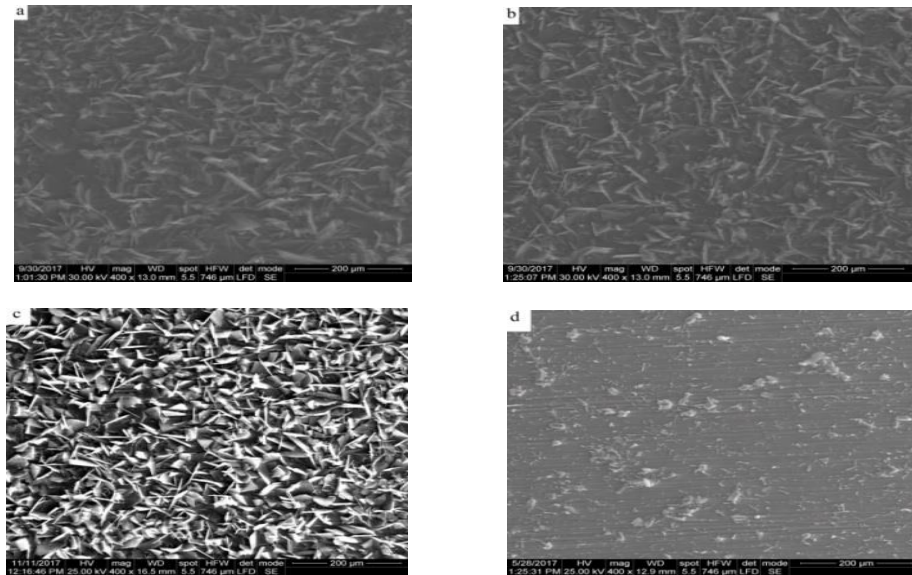


**Fig (1): Scanning electron microscope of surface morphology of a) HA b) HAP
c) HACa d) HAPCa**

Figs. 2(a, b) show the surface morphology of the coating obtained from hydroxyapatite after immersion in simulated body fluid (S.B.F) for different times, two weeks Fig 2 (a) and four weeks 2(b). The morphology image of figure 2(a) shows white flake-like particles with some nodules. Fig 2(b) shows white flake-like particles with some black plated area. The grain size is $10.49\ \mu\text{m}$ for two weeks and $6.99\ \mu\text{m}$ for four weeks.

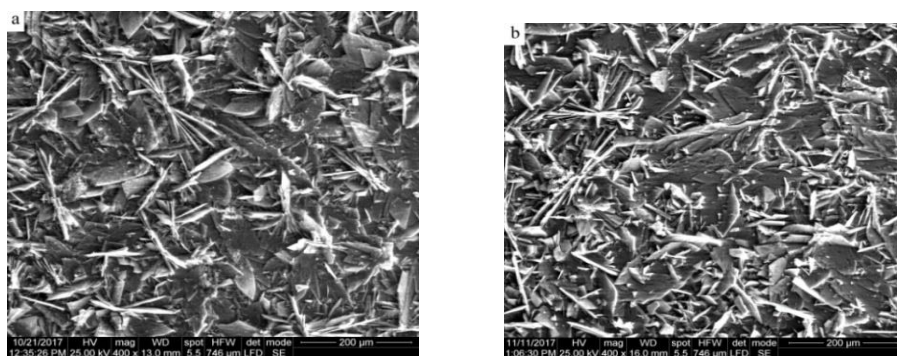


Fig (2): Scanning electron microscope of surface morphology of (HA) immersed in simulated body fluid for a) two weeks b) four weeks.

Figs. 3(a, b) show surface morphology of the coating bath (HAP) obtained after immersion of the specimens in simulated body fluid (SBF) solution for two and four weeks. All surface morphology of the dipping specimens 3(a, b) have flake-like particles with white and black flakes. The white colour

decreases from the two weeks to four weeks. The grain size is decreased by time of immersion from 8.77 μm to 7.74 μm for two weeks and four weeks respectively.

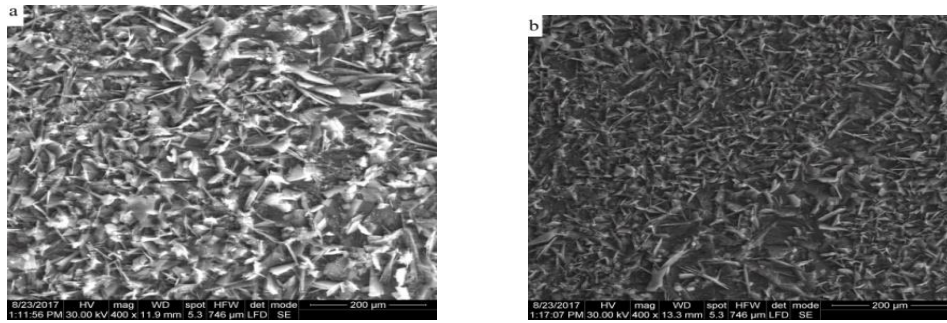


Fig (3): Scanning electron microscope of surface morphology of (HAP) immersed in simulated body fluid for a) two weeks b) four weeks.

Figs. 4 (a, b) show irregular shapes with grain size of $6.7 \mu\text{m}$ for two weeks and $5.2 \mu\text{m}$ for four weeks. Also white spots are appeared in all the dipped alloys (due to precipitation of Ca).

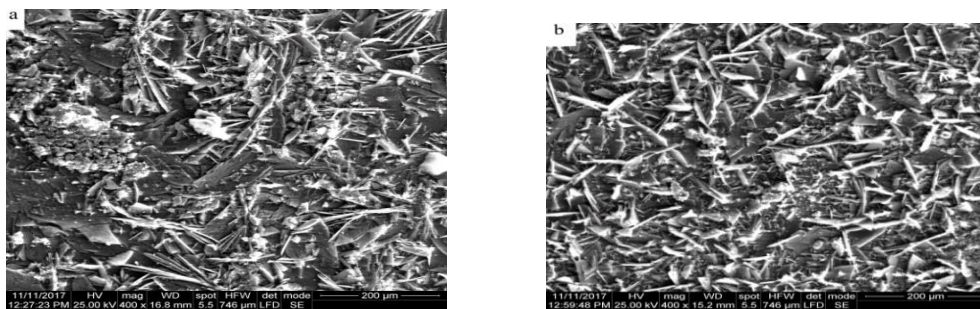


Fig (4): Scanning electron microscope of surface morphology of (HACa) immersed in simulated body fluid for a) two weeks b) four weeks.

An irregular shape is observed on all the tested surface species from both HAPCa with appearance of white colour. The white colour is decreased from figure 5 (a) to 5 (b) .(i.e. white spots decreases with time of immersion of HAPCa). The grain size is $7.74 \mu\text{m}$ for two weeks and $6.22 \mu\text{m}$ for four weeks.

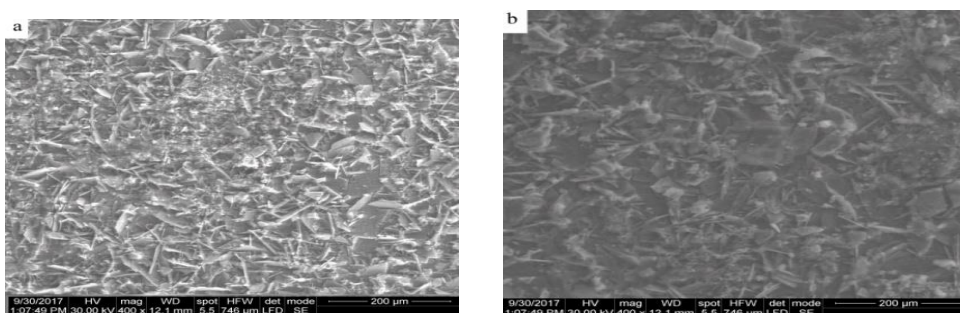


Fig (5): Scanning electron microscope of surface morphology of (HAPCa) immersed in simulated body fluid for a) two weeks b) four weeks.

The FTIR spectra of electrodeposited Mg-1%Zn alloy in HA, HAP, HACa and HAPCa are shown in Figs. 6(a-d). The most characteristic chemical groups in the FTIR spectra of HA, HAP, HACa and HAPCa are PO_4^{-3} , OH^{-1} and CO_3^{-2} . Phosphate group (PO_4^{-3}) forms intensive IR absorption at $560, 600 \text{ cm}^{-1}$ and at $1000-1100 \text{ cm}^{-1}$. Absorbed water band are relatively wide from 3600 to 2600 cm^{-1} with explicit peak at 870 and 880 cm^{-1} and more intensive peaks between 1460 and 1530 cm^{-1} . At $3531, 3541$ and 3543 cm^{-1} are due to stretching vibration which indicates the presence of water molecule as in Fig (6). The disappearance of the band 3541 cm^{-1} could be due to the substitution of OH^{-1} by NO_3^{-1} ions (direct substitution $2\text{OH}^{-1} \leftrightarrow \text{NO}_3^{-1}$) into HA, HAP, HACa and HAPCa. According to Figs. (6) a-d the layer precipitated on the surface contained NO_3^{-1} and PO_4^{-3} groups.

FTIR characterization of prepared samples confirms the formation of hydroxyapatite due to the presence of various modes of their functional groups.

The effect of immersion of the coated specimens by HA in S.B.F for two and four weeks is shown in figs. 7 (a, b). From the figures the functional groups NO_3^{-1} and PO_4^{-3} appeared i.e. formation of hydroxyapatite. The functional groups are shown in figures 8 (a, b), 9 (a, b) and 10 (a, b) for immersion in HAP, HACa and HAPCa for two and four weeks respectively.

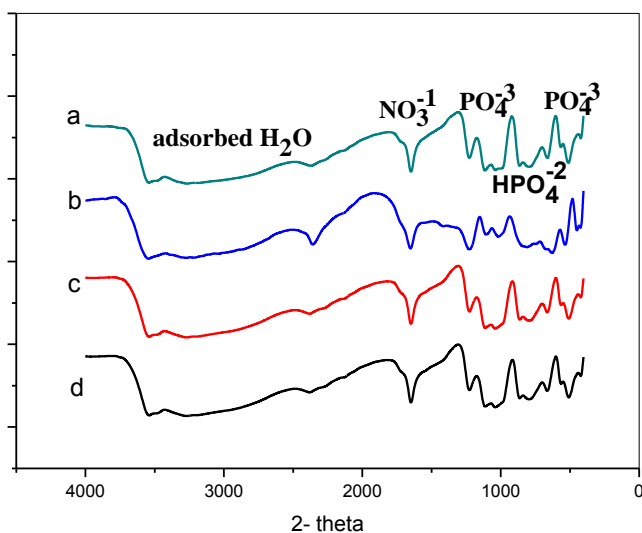


Fig (6): FTIR spectra for Mg-1%Zn as deposit form a) HA b) HAP c) HACa d) HAPCa bathes.

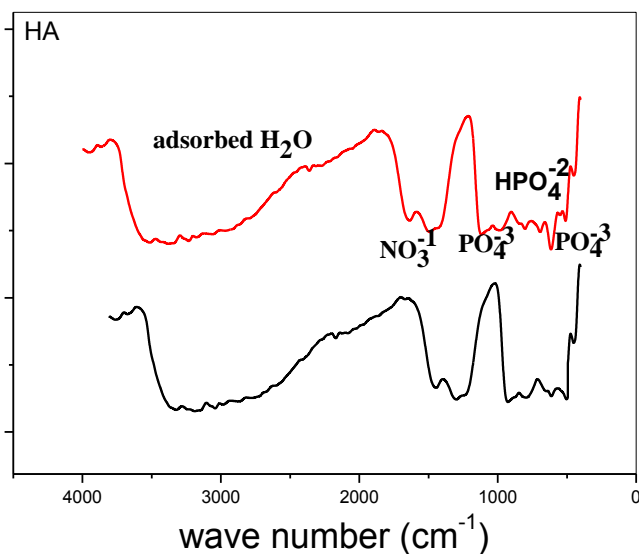


Fig (7): FTIR spectra for Mg-1%Zn (HA bath) immersed in S.B.F only for a) two weeks b) four weeks.

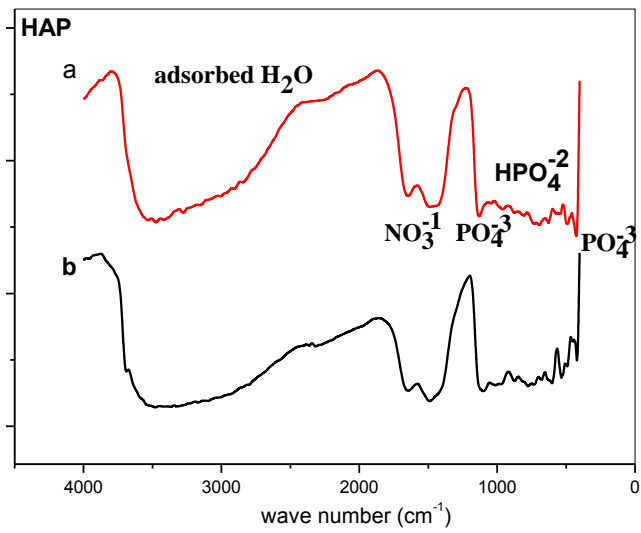


Fig (8): FTIR spectra for Mg-1%Zn (HAP bath) immersed in S.B.F only for a) two weeks b) four weeks.

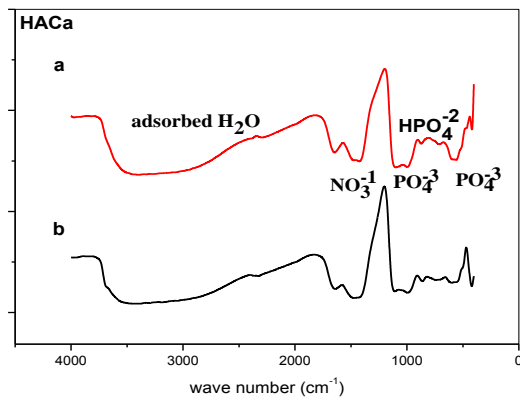


Fig (9): FTIR spectra for Mg-1%Zn (HACa bath) immersed in S.B.F only for a) two weeks b) four weeks.

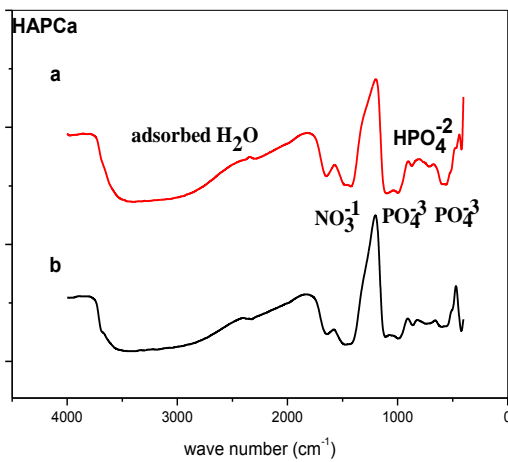


Fig (10): FTIR spectra for Mg-1%Zn (HAPCa bath) immersed in S.B.F only for a) two weeks b) four weeks.

The XRD patterns of as coated Mg-1%Zn alloy with bath HA, HAP, HACa and HAPCa are shown in figures 11(a-d). Fig 11(a) shows sharp peaks at 2θ equals 11.76, 34.42, 35.52 and 47.95 represent monoclinic calcium phosphate dihydrate $\text{CaHPO}_4 \cdot 2(\text{H}_2\text{O})$. Other sharp peaks with little heights also represent Brushite calcium phosphate dihydrate. At 2θ equal 63.18 represent hexagonal magnesium and also at 2θ equals 65, calcium oxide phase is shown. The average grain size of HA coating which is determined by Scherrer method is about 91 to 69.9 nm. Fig 11(b-d) represent the same phases (monoclinic calcium phosphate dihydrate, hexagonal magnesium and calcium oxide) but accompanied by small positional shifts towards higher or lower angles. The average grain size of the coat in bath HAP is 80-46 nm. N.B. All the coatings are crystalline in nature.

Fig 12(a) shows the EDAX analysis of the as deposit coating obtained before immersion in S.B.F of HA bath. Strong peaks of Ca, P, Mg and O elements are present.

Fig 12 (b-d) show the EDAX analysis of the as deposited samples in HAP, HACa and HAPCa without immersion in S.B.F. Also strong peaks reveal Ca, P, Mg and O elements.

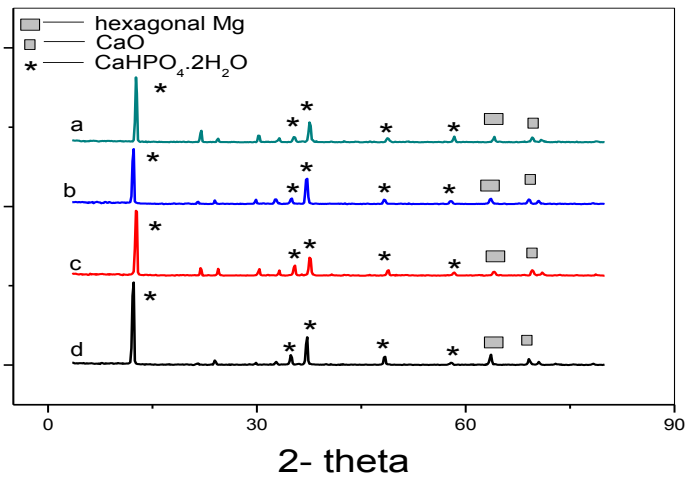


Fig (11): X-ray diffraction patterns of Mg-1%Zn as deposited from a) HA b) HAP c) HACa d) HAPCa bathes.

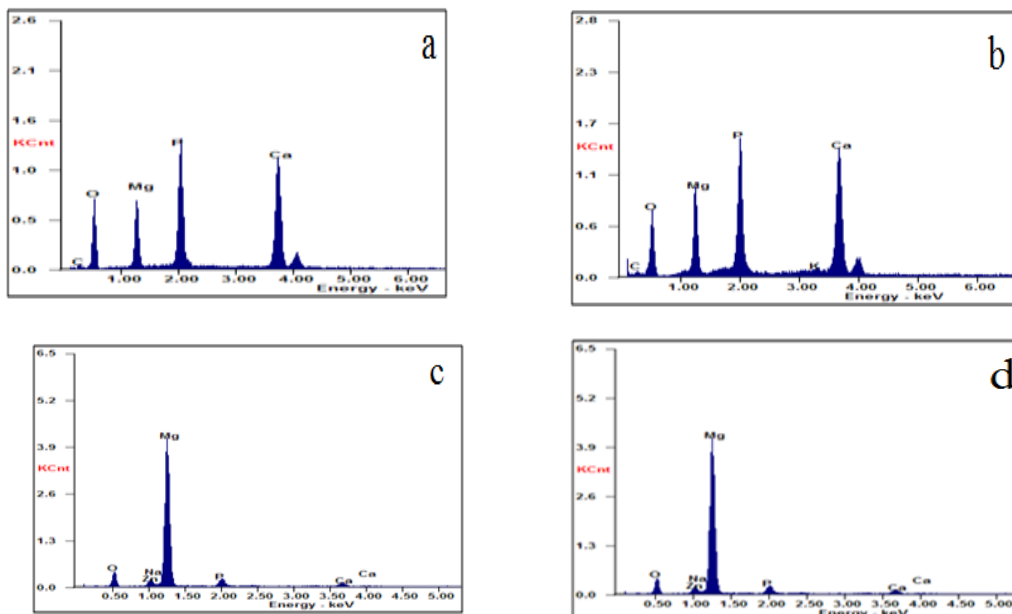


Fig (12): EDAX of Mg-1%Zn as deposited from a) HA b) HAP c) HACa d) HAPCa bathes.

X-ray diffraction patterns of the corrosion product from coated specimens with HA, HAP, HAPCa and HAPCa for two weeks and four weeks are shown in Figs. 13(a, b), Figs. 14(a, b), Figs. 15(a, b) and Figs. 16(a, b).

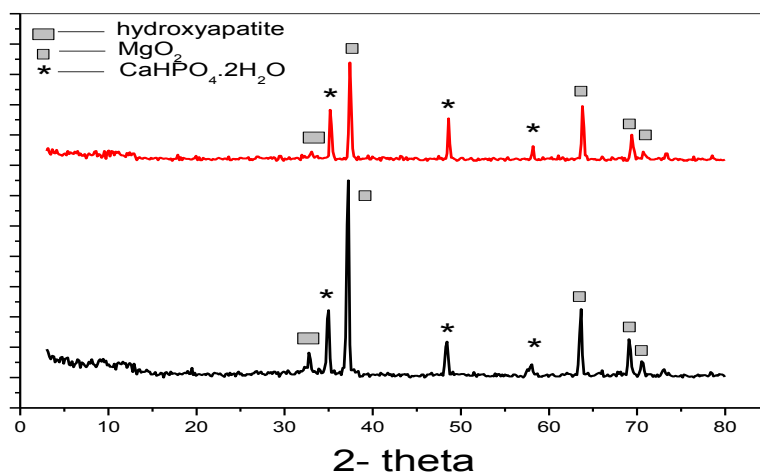


Fig (13): X-ray diffraction patterns of Mg-1%Zn as deposited from HA bath after immersion in S.B.F for a) two weeks and b) four weeks.

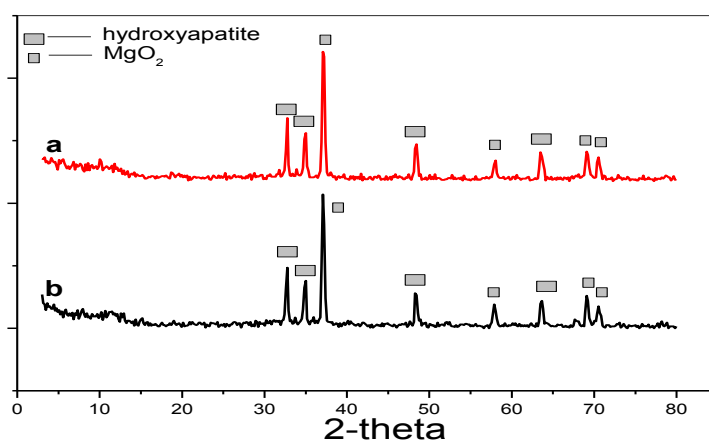


Fig (14): X-ray diffraction patterns of Mg-1%Zn as deposited from HAP bath after immersion in S.B.F for a) two weeks and b) four weeks.

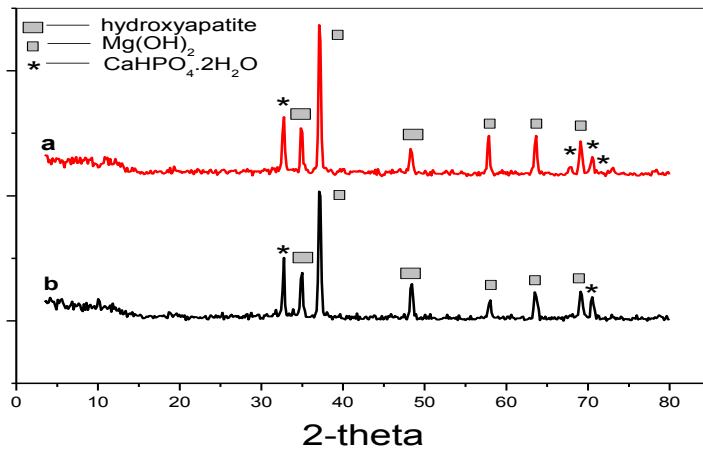


Fig (15): X-ray diffraction pattern of Mg-1%Zn as deposited from HACa bath after immersion in S.B.F for a) two weeks and b) four weeks.

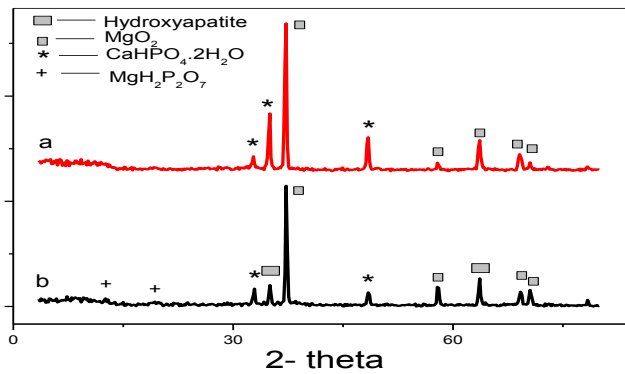


Fig (16): X-ray diffraction patterns of Mg-1%Zn (HACaP coat) after immersion in S.B.F for a) two weeks and b) four weeks.

Figs (17-20) represent the EDAX analysis of the corrosion product of coated specimens by HA, HAP, HACa and HAPCa after immersion in S.B.F for two and four weeks.

The EDAX analysis of the corrosion product from bath HA in case of immersion for two weeks reveal the presence of Cl, Mg, Ca, P and O elements. In agreement with X-ray diffraction since calcium hydrogen phosphate dihydrate $\text{CaHPO}_4 \cdot (\text{H}_2\text{O})_2$, hydroxyapatite $\text{Ca}_5(\text{PO}_4)_3(\text{OH})$ phases are present. X-ray diffraction of the corrosion products after four weeks give calcium hydrogen phosphate dihydrate $\text{CaHPO}_4 \cdot (\text{H}_2\text{O})_2$ and magnesium dioxide MgO_2 phases. With increasing of immersion time to four weeks, the peaks of Ca and P continued to increase and Mg peaks continued to decrease as shown in Fig 20(b). This continuous growing of HA with immersion of four weeks, obviously confirms the bioactivity of the coating.

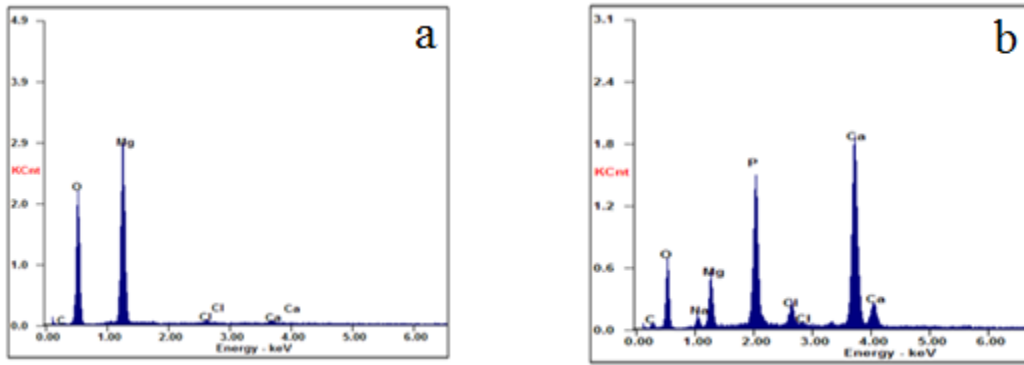


Fig (17): EDAX of Mg-1%Zn as deposited from HA bath for a) two weeks b) four weeks.

EDAX analysis for the corrosion products obtained from HAP bath coating after two weeks immersion fig. 18(a) reveal the presence of Cl, Mg, Ca, P and O elements in agreement with X-ray diffraction that the phases are hydroxyapatite $\text{Ca}_5\text{PO}_3(\text{OH})_2(\text{H}_2\text{O})$ and magnesium dioxide MgO_2 . In case of immersion of specimens in S.B.F for four weeks Fig 18(b), the coat reveals the presence of Ca, Mg and O elements. Also, in agreement with X-ray diffraction presence of MgO_2 and hydroxyapatite $\text{Ca}_5\text{PO}_3(\text{OH})_2(\text{H}_2\text{O})$ phases.

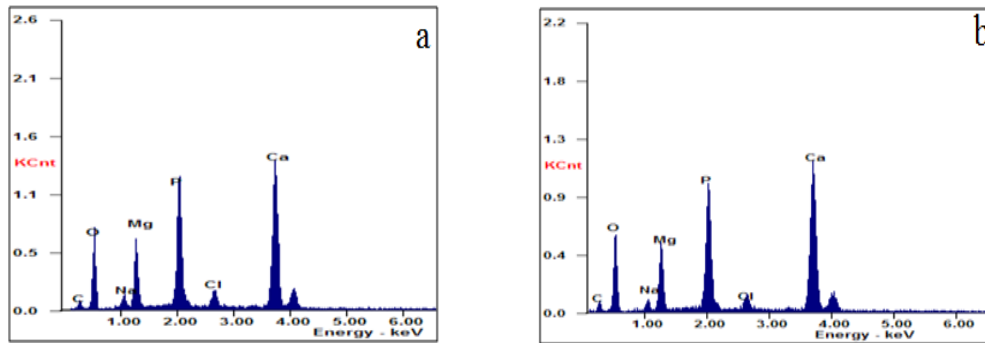


Fig (18): EDAX of Mg-1%Zn as deposited from HAP bath for a) two weeks b) four weeks.

It is observed from the EDAX spectrum of the coated specimens with bath HACa, after immersion of two weeks and four weeks in S.B.F that well resolved peaks corresponding to different elements Ca, P, O, Mg and Cl are present in figs. 19(a, b) and confirm the synthesis of hydroxyapatite $\text{Ca}_5(\text{PO}_4)_3(\text{OH})$, calcium hydrogen phosphate dihydrate $\text{CaHPO}_4(\text{H}_2\text{O})_2$ and $\text{Mg}(\text{OH})_2$ phases. In agreement with X-ray diffraction for two weeks immersion in the SBF. In case of dipping four weeks calcium hydrogen phosphate dihydrate and magnesium hydroxide phases are appeared. average grain size of the coat in bath HACa is 57.5-39.8 nm. A single unwanted peak of Na is observed which might be due to the foreign impurity.

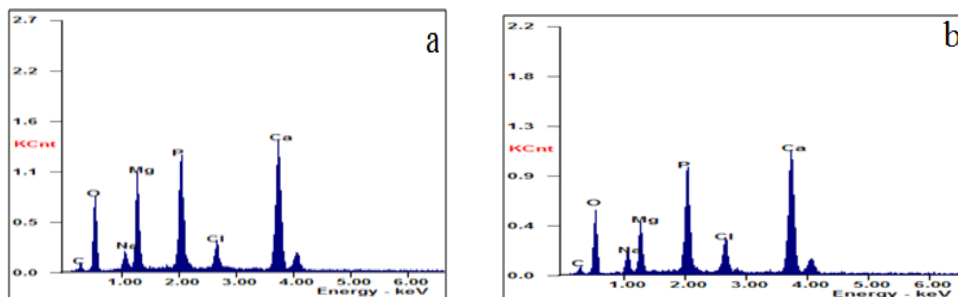


Fig (19): EDAX of Mg-1%Zn as deposited from HACa bath for a) two weeks b) four weeks.

Figs. 20 (a, b) show the EDAX results of the coating obtained from HAPCa after immersion in S.B.F solution for two and four weeks. Strong peaks of calcium (Ca), phosphorous (P), magnesium (Mg) and oxygen (O) and several small peaks are observed. The phases obtained from the XRD results of the coating after immersion in S.B.F for two weeks calcium hydrogen phosphate dihydrate $\text{CaHPO}_4(\text{H}_2\text{O})_2$ and MgO_2 phases are obtained. In case of immersion for four weeks, hydroxyapatite $\text{Ca}_5(\text{PO}_4)_3(\text{OH})$, magnesium hydrogen phosphate $\text{MgH}_2\text{P}_2\text{O}_7$ and MgO_2 phases appears. average grain size of the coat in bath HAPCa is 48.4-36.8 nm.

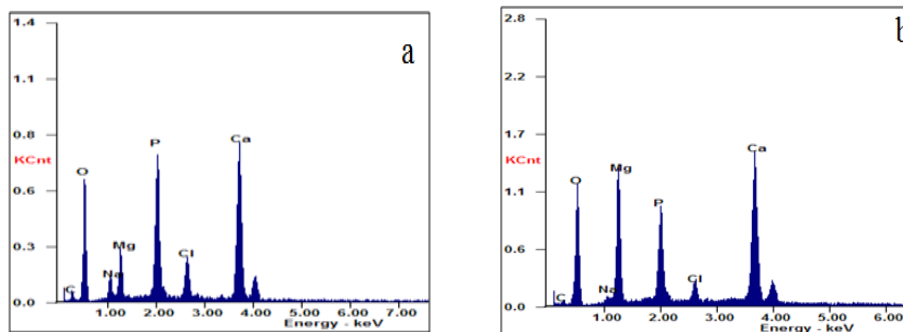


Fig (20): EDAX of Mg-1%Zn as deposited from HAPCa bath for a) two weeks b) four weeks.

Potentiodynamic polarization studies:

Fig. (21) shows Potentiodynamic polarization curves of the Mg-1%Zn alloy substrate coated with HA, HAP, HACa and HAPCa in SBF. The corrosion potential (E_{corr}), corrosion current density (I_{corr}) and the anodic and cathodic Tafel constants (β_a , β_c) are extracted directly from the Potentiodynamic polarization curves using Tafel extrapolation and linear polarization methods [M.H Fathi et al].

The polarization resistance (R_p) is calculated by Stern- Geary equation (Eq. (1) [Hongping Duan et al, Soha A et al])

$$R_p = \frac{\beta_a \times \beta_c}{2.3 \times i_{\text{corr}} (\beta_a + \beta_c)} \quad \text{Eq. (1)}$$

All the electrochemical parameters calculated from Tafel plots are listed in Table (2). It is shown that the treated samples with a lower I_{corr} , positive E_{corr} and higher R_p have a good corrosion resistance. The corrosion resistance of samples is improved after the surface coating by HA, HAP, HACa and HAPCa. By comparing the data E_{corr} and I_{corr} of coated sample HAPCa are -1.520 v and $1.25 \times 10^{-4} \text{ A/cm}^2$ respectively. E_{corr} (-1.722) of coated sample with HA is slightly less than that of coated by HAPCa, while the I_{corr} ($7.94 \times 10^{-4} \text{ A/cm}^2$) is reduced. In addition, R_p (553.68) of coat HAPCa is reduced to 116.41 for coat HA. It is indicated that HAPCa treated sample has higher corrosion resistance than HACa, HAP and HA. The refinement of the microstructure is good for improving the corrosion resistance of the coated Mg-1%Zn. The corrosion protection of coated samples in SBF follows the sequence HAPCa > HACa > HAP > HA.

Table (3): the corrosion kinetic parameters E_{corr} , I_{corr} , C_R and R_p determined from the polarization curves in the Tafel region for the four bathes HA, HAP, HACa and HAPCa in simulated body fluid.

Bath	E_{corr} (V)	I_{corr} (A/cm^2)	C_R	β_a (V)	β_c (V)	R_p
------	-----------------------	---------------------------------------	-------	---------------	---------------	-------

HA	-1.722	7.94×10^{-4}	5.50×10^{-4}	0.270	1.000	116.41
HAP	-0.858	5.62×10^{-4}	3.640×10^{-4}	0.225	0.860	152.15
HACa	-1.586	4.57×10^{-4}	3.160×10^{-4}	0.230	0.810	170.04
HAPCa	-1.520	1.25×10^{-4}	0.860×10^{-4}	0.200	0.780	553.68

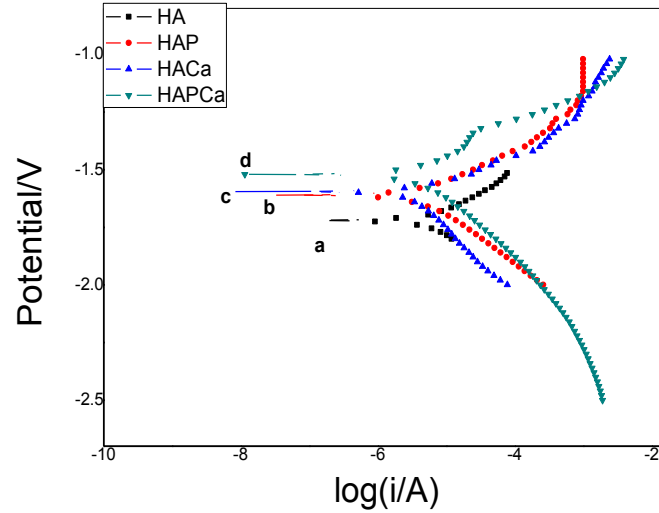


Fig. (21): Potentiodynamic polarization curves of the Mg-1%Zn alloy substrate coated with a) HA b) HAP c) HACa and d) HAPCa in SBF.

Fig. (22) shows Potentiodynamic polarization curves of a coat substrate by bath HA before and after immersion in SBF for two and four weeks. The corrosion potential of the substrate coat -1.722v

For four weeks show the best corrosion resistance than which immersed for two weeks and finally the coated substrate. Table (4) shows the corresponding E_{corr} and I_{corr} for the pervious results.

The same results are observed for the other bathes as shown in Figs. (23, 24, 25) and tables (5,6, 7).

Table (4): the corrosion kinetic parameters E_{corr} , I_{corr} , C_R and R_P determined from the polarization curves in the Tafel region for HA bath in simulated body fluid.

Bath	E_{corr} (V)	I_{corr} (A/cm^2)	C_R	β_a (V)	β_c (V)	R_P ($\Omega \cdot \text{cm}^2$)
HA	-1.722	7.94×10^{-4}	5.50×10^{-4}	0.270	1.000	116.41
HA(2 weeks)	-1.298	5.01×10^{-4}	3.470×10^{-4}	0.220	0.772	146.33
HA (4 weeks)	-1.248	1.77×10^{-4}	1.220×10^{-4}	0.160	0.630	313.42

Table (5): the corrosion kinetic parameters E_{corr} , I_{corr} , C_R and R_P determined from the polarization curves in the Tafel region for HAP bath in simulated body fluid.

Bath	E_{corr} (V)	I_{corr} (A/cm ²)	C_R	β_a (V)	β_c (V)	R_p
HAP	-1.611	5.62×10^{-4}	3.640×10^{-4}	0.225	0.860	152.15
HAP (2weeks)	-1.290	3.98×10^{-4}	2.750×10^{-4}	0.200	0.760	172.96
HAP (4 weeks)	-1.285	0.61×10^{-4}	0.422×10^{-4}	0.144	0.600	827.71

Table (6): the corrosion kinetic parameters E_{corr} , I_{corr} , C_R and R_p determined from the polarization curves in the Tafel region for HACa bath in simulated body fluid.

Bath	E_{corr} (V)	I_{corr} (A/cm ²)	C_R	β_a (V)	β_c (V)	R_p
HACa	-1.586	4.57×10^{-4}	3.160×10^{-4}	0.230	0.810	170.04
HACa (2weeks)	-1.260	3.54×10^{-4}	0.420×10^{-4}	0.192	0.690	184.48
HACa (4 weeks)	-0.585	0.467×10^{-4}	0.323×10^{-4}	0.130	0.588	991.17

Table (7): the corrosion kinetic parameters E_{corr} , I_{corr} , C_R and R_p determined from the polarization curves in the Tafel region for HAPCa bath in simulated body fluid.

Bath	E_{corr} (V)	I_{corr} (A/cm ²)	C_R	β_a (V)	β_c (V)	R_p
HAPCa	-1.520	1.25×10^{-4}	0.860×10^{-4}	0.200	0.780	553.68
HAPCa (2weeks)	-1.248	0.39×10^{-4}	0.100×10^{-4}	0.180	0.640	1566.19
HAPCa (4 weeks)	-0.184	0.150×10^{-4}	0.103×10^{-4}	0.100	0.540	2445.65

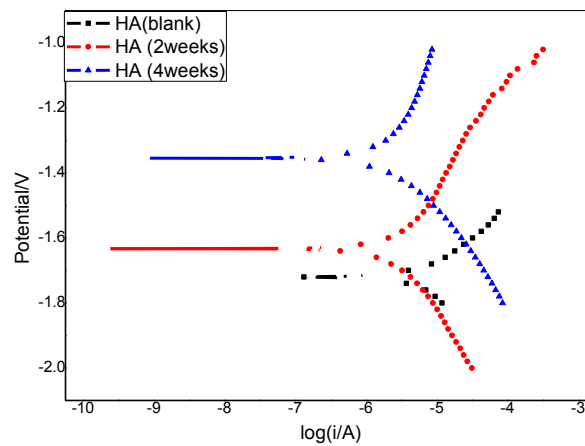


Fig. (22): Potentiodynamic polarization curves of the Mg-1%Zn alloy substrate coated with HA bath in SBF a) blank b) 2 weeks c) 4 weeks.

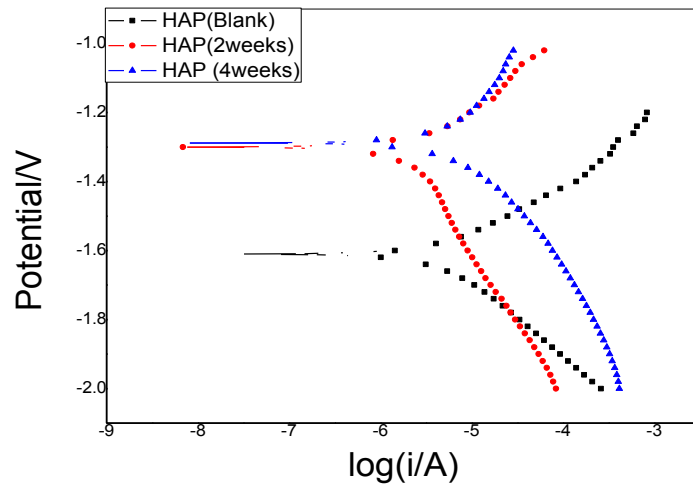


Fig. (23): Potentiodynamic polarization curves of the Mg-1%Zn alloy substrate coated with HAP bath in SBF a) blank b) 2 weeks c) 4 weeks.

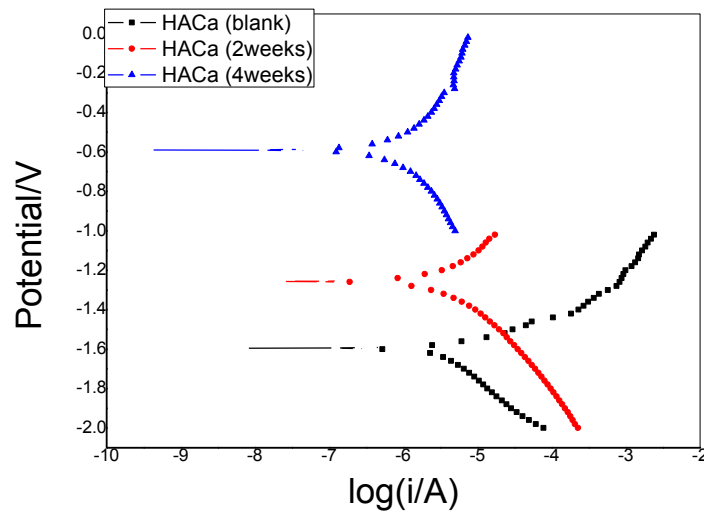


Fig. (24): Potentiodynamic polarization curves of the Mg-1%Zn alloy substrate coated with HACa bath in SBF a) blank b) 2 weeks c) 4 weeks.

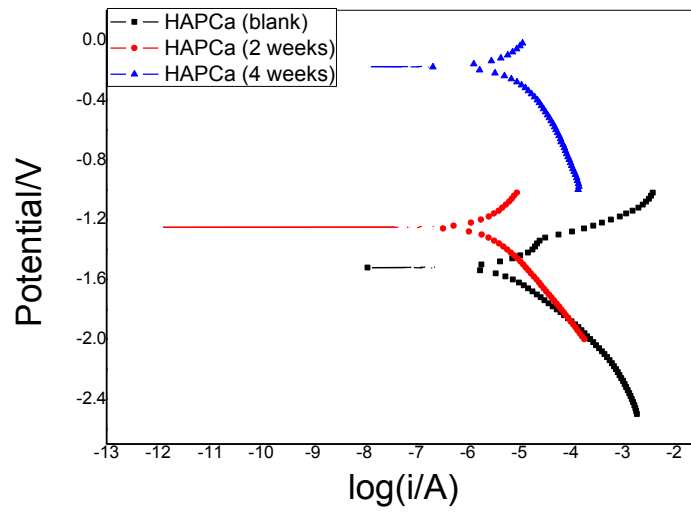


Fig. (25): Potentiodynamic polarization curves of the Mg-1%Zn alloy substrate coated with HAPCa bath in SBF a) blank b) 2 weeks c) 4 weeks.

References:

- A. Farzadi, F. Bakhshi, M. Solati-Hashjin, M. Asadi-Eydiv, N. Azuan abu Osman. Magnesium incorporated hydroxyapatite: Synthesis and structural properties characterization. *Ceramics International*. 2014, 40 , 6021-6029.
- D. Vojt'ich, J. Kub'asek, J. Capek and I. Posp'isilov'a, *Mater. Technol.*, 2015, 49, 877–882.
- D. Vojtech, J. Kub'asek, J. Ser'ak and P. Nov'ak, *Acta Biomater.*, 2011, 7, 3515–3522.
- G. Hu, L. Zeng, H. Du, X. Fu, X. Jin, M. Deng, Y. Zhao, X. Liu. The formation mechanism and bio-corrosion properties of Ag/HA composite conversion coating on the extruded Mg-2Zn-1Mn-0.5Ca alloy for bone implant application. *Surface and Coatings Technology*. 2017, 325, 127-135.
- Hongping Duan, Chuanwei Yan, Fuhui Wang, Effect of electrolyte additives on performance of plasma electrolytic oxidation films formed on magnesium alloy AZ91D, *Electrochimica Acta*, 2007, 52, 3785-3793.
- J. Kubasek and D. Vojtech, 21st International Conference on Metallurgy and Materials 2012, 1355–1361.
- J.A.del Valle, M.Fernandez-Lorenzo, M.C.Garcia-Alonso, O.A.Ruano, M.L.Escudero. Corrosion behaviour of AZ31 magnesium alloy with different grain sizes in simulated biological fluids. *Acta Biomaterialia*. 2010, 6, 1763-1771.
- Jamesh, M., Kumar, S., & Sankara Narayanan, T. S. N. Electrodeposition of hydroxyapatite coating on magnesium for biomedical applications. *Journal of Coatings Technology and Research*, 2011, 9, 495–502.
- M. M. Alves, T. Prošek, C. F. Santos, M. F. Montemora. Evolution of the in vitro degradation of Zn–Mg alloys under simulated physiological conditions. *The Royal Society of Chemistry RSC Adv*. 2017, 7, 28224.
- M. S. Dambatta, S. Izman, D. Kurniawan, S. Farahany, B. Yahaya and H. Hermawan, *Mater. Des.*, 2015, 85, 431–437.
- M.H Fathi, M Salehi, A Saatchi, V Mortazavi, S.B Moosavi, In vitro corrosion behavior of bioceramimetallic, and bioceramic–metallic coated stainless steel dental implants, *Dental Materials*, 2003, 19, 188-198.
- S.M. Abd El Hallem, Ghayad, M. Eisaa, N. Nassif, M.A.Shoeib, H. Soliman. Effect of Ultrasonic and Mechanical Vibration on the Corrosion Behavior of Mg-3Zn-0.8Ca Biodegradable Alloy. *Int. J. Electrochem*. 2014, 9, 2005 – 2015.
- Soha A. Abdel-Gawada, Madiha A. Shoeib, Corrosion studies and microstructure of Mg–Zn–Ca alloys for biomedical applications, *Surfaces and Interfaces*, 2019, 14, 108-116.
- Wenhao Wang, Kelvin W.K. Yeung. Bone grafts and biomaterials substitutes for bone defect repair. *Bioactive Materials* 2017, 2(4), 224-247.
- Y. Song, D. Shan, R. Chen, F. Zhang, En-HouHan. Biodegradable behaviors of AZ31 magnesium alloy in simulated body fluid. *Materials Science and Engineering,C*. 2009, 29, 1039-1045.
- Y. Xiong, Q. Hu, R. Song, X. Hu. LSP/MAO composite bio-coating on AZ80 magnesium alloy for biomedical application. *Materials Science and Engineering:C*. 2017, 75, 1299-1304.
- Y. Yan, H. Cao, Y. Kang, K.Yu, T. Xiao, J. Luo, Y. Deng, H. Fang, H. Xiong, Y. Dai, M. Alvarez-Lopez, M. Dolores. Effects of Zn concentration and heat treatment on the microstructure, mechanical properties and corrosion behavior of as-extruded Mg-Zn alloys produced by powder metallurgy. *Journal of Alloys and Compounds*, 2017, 693, 1277-1289.

الملخص العربي

تتكون معظم جراحات العظام التقليدية المستخدمة لالتحام الكسور من سرائح معدنية لا تتفاعل مع المحلول الحيوي بالجسم. هذه السرائح المعدنية المختارة يجب أن تظهر صلابة عالية ومقاومة جيدة للتآكل.

حديثاً لتجنب استخراج السرائح المعدنية من بعض الأجسام التي لها حساسية ضدها اتجه العلماء الى استخدام سرائح لها قابلية للتحلل في محلول الجسم. وهذه تتكون من مواد غير سامة والتي يعاد امتصاصها بالجسم بعد فترة زمنية معقولة.

ولقد استخدمنا في دراستنا الحالية سبيكة ماغنسيوم - ١% زنك حيث أن عنصر الزنك يحسن الخواص الميكانيكية للماغنسيوم وليس له أي آثار جانبية على الجسم والمغنسيوم لديه خاصية تآكل ضعيفة في محلول الجسم وقمنا في هذه الدراسة بتحسين سبيكة ماغنسيوم - ١% زنك من حيث مقاومتها للتآكل في محلول محاكي لمحلول الجسم عن طريق استخدام الطلاء الكهربى لهذه السبيكة في حمام من الهيدروكسى اباتيت (HA) ثم أضيف الى حمام الهيدروكسى اباتيت كمية زائدة من الفسفور على هيئة امونيوم داى هيدروجين فوسفات ($\text{NH}_4\text{H}_2\text{PO}_4$) ليكون حمام (HAP) ، وايضا تم استخدام حمام ثالث من الحمام الاول مضاف اليه كمية زائدة من الكالسيوم في صورة نترات الكالسيوم $\text{Ca}(\text{NO}_3)_2$ وه (HACa) واخيرا حمام (HAPCa) وهو عبارة عن حمام الهيدروكسى اباتيت مضاف اليه كمية زائدة من كل من الفوسفور والكالسيوم من املاح ($\text{NH}_4\text{H}_2\text{PO}_4, \text{Ca}(\text{NO}_3)_2$)

وقد اثبتت النتائج أن مقاومة التآكل لسرائح ماغنسيوم - ١% زنك في محلول يحاكي محلول الجسم تتبع الترتيب التالي



مدرس مساعد / مروة محمد محمد اسماعيل
قسم الكيمياء - كلية البنات - جامعة عين شمس

استاذ مساعد/ أميمة رمضان محمد خليفة
قسم الكيمياء - كلية البنات - جامعة عين شمس

استاذ مساعد/ انشراح عبد الوهاب عبد الحميد
قسم الكيمياء - كلية البنات - جامعة عين شمس

استاذ مساعد/ عائشة كساب عبد العزيز كساب
قسم الكيمياء - كلية البنات - جامعة عين شمس